Fermi National Accelerator Laboratory

FERMILAB-Pub-92/284-E

A Dalitz Plot Analysis of D→Kππ Decays

J.C. Anjos et al
The E691 Collaboration

Fermi National Accelerator Laboratory
P.O. Box 500, Batavia, Illinois 60510

November 1992

Submitted to *Physical Review Letters*

Operated by Universities Research Association Inc. under Contract No. DE-AC02-76CHO3000 with the United States Department of Energy

Disclaimer

A Dalitz plot analysis of D→Kππ decays

J. C. Anjos,[3] J. A. Appel,[6] A. Bean,[1] S. B. Bracker,[11] T. E. Browder,[1,a] L. M. Cremaldi,[7]
G. C. Danner,[9] J. Duboscq,[1,b] J. R. Elliott,[5,c] C. O. Escobar,[10] M. C. Gibney,[5,d] A. S. Gordon,[9,e]
G. F. Hartner,[11] P. E. Karchin,[12] B. R. Kumar,[11] M. J. Losty,[8] G. J. Luste,[11] P. M. Mantsch,[6]
J. F. Martin,[11] S. McHugh,[1] S. R. Menary,[11,f] R. J. Morrison,[1] T. Nash,[6]
P. Ong,[11] J. Pinfold,[2] G. Punkar,[1,g] M. V. Purohit,[9] J. R. Raab,[1,h] W. R. Ross,[12]
A. F. S. Santoro,[3] A. L. Shoup[4,i] J. S. Sidhu,[2,j] K. Sliwa,[6,k] M. D. Sokoloff,[4]
M. H. G. Souza,[3] M. E. Streetman,[6] A. B. Stundžia,[11] W. D. Volkmuth,[9] M. S. Witherell[1]

[1]University of California, Santa Barbara, CA 93106, USA

[2]Carleton University, Ottawa, Ontario K1S 5B6, Canada

[3]Centro Brasileiro de Pesquisas Físicas, Rio de Janeiro, Brazil

[4]University of Cincinnati, Cincinnati, OH 45221, USA

[5]University of Colorado, Boulder, CO 80309, USA

[6]Fermi National Accelerator Laboratory,* Batavia, IL 60510, USA

[7]University of Mississippi, University, MS 38677, USA

[8]National Research Council, Ottawa, Ontario K1A OR6, Canada

[9]Princeton University, Princeton, NJ 08544, USA

[10]Universidade de São Paulo, São Paulo, Brazil

[11]University of Toronto, Toronto, Ontario M5S 1A7, Canada

[12]Yale University, New Haven, CT 06511, USA

Decays of the D^0 meson to $K^-\pi^+\pi^0$ and $\overline{K}^0\pi^+\pi^-$ and of the D^+ to $K^-\pi^+\pi^+$ have been analysed for resonant substructure. We present results on the amplitudes and phases of each decay mode and compare the results with other measurements.

We confirm the highly non-resonant nature of the D^+ to $K^-\pi^+\pi^+$ decays. There is general agreement with theoretical models for the branching ratios measured.

13.25.+m, 14.40.Ev

Hadronic decays of charmed particles have been a subject of much study in the past few years as new information from experiments has become available. Theorists have attempted to understand these data and have made predictions concerning hadronic decays.[1,2] Since the charm quark is not very heavy, charm hadrons decay mainly into two, three and four particles. Here we examine three body decays of the D^0 meson to $K^-\pi^+\pi^0$ and $\overline{K}^0\pi^+\pi^-$ and of the D^+ to $K^-\pi^+\pi^+$ to determine the fractions into two body modes and the relative phases of the decay amplitudes. In this paper we implicitly include decays of antiparticles.

The data sample comes from the fixed-target photoproduction experiment E691 done at Fermilab during 1985 and described elsewhere.[3] The experiment recorded 100 million events from which approximately 10,000 charm particle decays were reconstructed. We first describe the reconstruction and analysis common to all three modes and then describe the event selection specific to individual modes.

Events were selected by requiring that the D meson decay tracks satisfy a vertex hypothesis with a χ^2 per degrees of freedom (χ^2/DF) less than 3.5, that the reconstructed candidate D point back to within 80 microns of the primary vertex in the transverse plane and that the primary vertex itself have a $\chi^2/\mathrm{DF} < 6$. We further required that the separation of the primary and secondary vertices along the beam direction divided by the error on this quantity be larger than 6. In all three decay modes we required that the charged tracks go through at least one of our two analysis magnets and that each track have a particle identification probability based on Čerenkov information of at least 50%.

In the case of the $D^+ \rightarrow K^-\pi^+\pi^+$ decays, we required that there be no other tracks within 100 μm of the secondary vertex in the transverse direction. A signal of 4149 ± 79 events results (fig. 1a). In order to minimize backgrounds in both the D^0 decay modes, we select only those D^0 candidates which are products of D^{*+} decays.

The pion from the D^{*+} decay was required to satisfy the same requirements as are the other charged tracks. In the $D^0 \rightarrow \overline{K}^0\pi^+\pi^-$ mode the Q value of the candidate D^{*+} decays was allowed to be within $\pm$ 1.5 MeV of the expected value and in the $D^0 \rightarrow K^-\pi^+\pi^0$ mode to be within $\pm$ 2.5 MeV of the expected value. The K^0_S decay tracks are required to go through both magnets, have a product particle identification probability greater than 5%, a distance of closest approach of less than 5 mm (and 100μm for the small fraction of K^0_S that decay before the precision silicon vertex detector). The K^0_S decay volume was restricted to end upstream of the first magnet. The reconstructed K^0_S mass was required to lie between 480 and 514 MeV/c^2. In the $K^-\pi^+\pi^0$ mode the π^0 particles were required to have at least 8 GeV in energy and lie outside the "pair-plane", a $\pm$3 cm band in our electromagnetic calorimeter where the entire background of e^+e^- pairs from low energy bremsstrahlung photons appears. The signals for the $D^0 \rightarrow \overline{K}^0\pi^+\pi^-$ mode (174 $\pm$ 20 events) and for the $D^0 \rightarrow K^-\pi^+\pi^0$ mode (317 $\pm$ 20 events) are shown in figs. 1b and 1c.

Our technique for creating and fitting Dalitz plots is described here using the high statistics mode $D^+ \rightarrow K^-\pi^+\pi^+$ as an illustration. The same technique was used in all three modes. For the displayed D^+ Dalitz plot, we randomly order the two identical pions; the fitting functions are symmetrized, so it does not affect the results. The Dalitz plot for the region containing the signal is shown in fig. 2a and for events in the background region is shown in fig. 2b. Events are constrained to lie within the Dalitz plot boundary by forcing the D^+ candidate mass to 1.8693 GeV/c^2 and the D^0 candidate mass to 1.8645 GeV/c^2 (ref. 4) by scaling the momenta of the decay particles. These constraints reduce the smearing of events within the Dalitz plot. In the $D^+ \rightarrow K^-\pi^+\pi^+$ and $D^0 \rightarrow \overline{K}^0\pi^+\pi^-$ modes all three decay momenta were scaled by the same factor, while for the $D^0 \rightarrow K^-\pi^+\pi^0$ mode we used the additional constraint of the π^0 mass and modified only the energies of the π^0 decay photons. The fraction of

background under the signal (b) is determined from the number of events in the wings of the peak in the mass plot. The background is parameterized free of any specific functional form by subdividing the allowed Dalitz plot kinematic region iteratively into smaller squares until the number of events in each square is too small or the area of the square is sufficiently small (adaptive binning). In this way we can accurately reproduce the background distribution in a model independent way for both high and low statistics samples. The simulated background for the $D^+ \to K^-\pi^+\pi^+$ mode is shown in fig. 2c. The acceptance over the Dalitz plot is determined from a Monte Carlo simulation. The r.m.s variation was found to be 10% of the mean for the $D^+ \to K^-\pi^+\pi^+$ mode, 45% of the mean in the $D^0 \to K^-\pi^+\pi^0$ mode and 95% of the mean in the $D^0 \to \overline{K}^0\pi^+\pi^-$ mode. We parameterized the acceptance in two different ways: as a simple bilinear function of the two Dalitz plot variables and using the adaptive binning scheme described above for the background. In fig. 3 we show the signal region Dalitz plots for the D^0 modes (note that the signal/background ratio in these modes is much better than in the D^+ case for our choice of cuts).

The two variables chosen to define the axes of the Dalitz plot are the squares of the invariant masses of the two $K\pi$ combinations. If these are denoted as x and y, the signal is assumed to be distributed as a uniform non-resonant term plus a sum over all resonances:

$$S(x,y) = |1 + \sum_{k=1}^{n} c_k \exp(i\theta_k) BW_k(x,y) ANG_k(x,y)|^2$$

where BW_k is a normalized Breit-Wigner function and ANG_k descibes the angular distribution for the k^{th} resonance. Since we fit only the shape and since there is always one arbitrary phase, the function has the non-resonant amplitude fixed at 1 and the non-resonant phase fixed at 0. We fitted the data to the form $bB(x,y) + (1-b)S(x,y)$, where B is the background function described above and b is the fraction

of background events as determined from the $K\pi\pi$ mass spectrum.

In the D^+ case, the resonances tried were the $K^{*0}(892)$, $K^{*0}(1410)$, $K_0^{*0}(1430)$, $K_2^{*0}(1430)$, $K^{*0}(1680)$, $K_3^{*0}(1780)$ and the $K_4^{*0}(2045)$. In the $D^0 \rightarrow K^-\pi^+\pi^0$ mode we tried to fit for the $K^{*0}(892)$, $K^{*-}(892)$, $\rho^+(770)$, $K^{*0}(1410)$, $K^{*-}(1410)$, $K_0^{*0}(1430)$, $K_0^{*-}(1430)$, $K_2^{*0}(1430)$, $K_2^{*-}(1430)$, $K^{*0}(1680)$, $K^{*-}(1680)$, $K_3^{*0}(1780)$, $K_3^{*-}(1780)$, $K_4^{*0}(2045)$, $K_4^{*-}(2045)$ and the $\rho_3^+(1690)$. In the $D^0 \rightarrow \overline{K}^0\pi^+\pi^-$ mode we tried to fit for the $K^{*-}(892)$, $\rho^0(770)$, $K^{*-}(1410)$, $K_0^{*-}(1430)$, $K_2^{*-}(1430)$, $K^{*-}(1680)$, $K_3^{*-}(1780)$, $K_4^{*-}(2045)$, $\omega(783)$, $f_0(975)$, $f_2(1270)$, $f_0(1400)$ and the $\rho_3(1690)$. We obtained the best values of the parameters c_k and θ_k by the maximum likelihood method in a simultaneous fit to all resonances listed above and the non-resonant contribution and background. Resonances whose fit fraction fell below 2% or was less than a 3 standard deviation effect were dropped from the final fit. The projections onto the two or three possible axes and the results of the fit described above are shown in figures 4a, 4b and 4c for the three different modes.

The results are summarized in tables I, II and III and include the contributions of all resonances which contribute a signal of at least three standard deviations. The fit fraction is determined by integrating each resonance individually over the area of the Dalitz plot and dividing by the integral of $S(x,y)$. The branching ratio is determined by multiplying the fit fraction by the PDG[4] value for the branching ratio in the 3-body final state and dividing by the relevant branching ratio of the resonance. The statistical errors on the branching ratios listed in the last column include the error on the fit fraction and the error on the branching ratio for the mode as reported by the particle data group (PDG).[4]

Systematic errors are quoted on the branching ratios and are a quadratic sum of the errors from three possible sources. First, the change observed by dropping resonances from the fit which contributed little to the fit fraction is an estimate of

the stability of the fitting procedure. Next, we estimate the accuracy of the Monte Carlo simulation. This is particularly important for the modes involving a π^0 or a K^0_S. As the second systematic error we consider the change in results after removing, from both data and Monte Carlo, events with a π^0 below 12 GeV or a K^0_S below 10 GeV (roughly 10% of our data). Finally, we consider the difference in results using the two different procedures for acceptance corrections described above as the third systematic error. The first two errors described are by far the largest sources of uncertainty, the third being always 1% or less of the corresponding branching ratio. Among other sources of systematic error considered but judged to be too small is any residual error after smearing is corrected for, event by event.

In conclusion, we find that in the $D^+ \rightarrow K^-\pi^+\pi^+$ decay the major contribution to the signal is from the non-resonant mode while for the D^0 decays the resonances dominate, in particular the K^* (892) and the ρ (770). Our results are consistent with previous measurements[5] by the Mark III collaboration listed in table IV. We allowed for more resonances in the fit to the $D^+ \rightarrow K^-\pi^+\pi^+$ decays than were used in ref. 5 (see also the analysis of Mark III data in ref. 6). Still, it is clear that the non-resonant mode dominates this channel, making it unique among the $D \rightarrow K\pi\pi$ decays. We note that the $D^0 \rightarrow K^{*-}\pi^+$ branching ratios measured in the two different final states (see table IV) are consistent with each other and that the branching ratio for $D^+ \rightarrow \overline{K}^*(1680)^0\pi^+$ is not inconsistent with our results in 4-body decay modes[7]. Combining the two results yields a branching ratio of $3.02 \pm 0.53\%$. This result can be combined with the decay rates for the modes $D^+ \rightarrow \overline{K}^{*0}\pi^+$ and $D^0 \rightarrow \overline{K}^{*0}\pi^0$ to yield the isospin amplitudes in $D \rightarrow K^*\pi$ decays and their phase difference. We measure $|A_{1/2}| = (3.50 \pm 0.26) \times 10^5/\sqrt{s}$, $|A_{3/2}| = (0.79 \pm 0.09) \times 10^5/\sqrt{s}$, $|A_{1/2}/A_{3/2}| = (4.46 \pm 0.65)$ and $(\delta_{1/2} - \delta_{3/2}) = (64^\circ \pm 22^\circ)$. The ratio of amplitudes and the phase difference agree with the values obtained by Mark III[5]. It is interesting that our measurements are

also in good agreement with the values measured for $D \to K\pi$ decays.[5]

We also compare our results with predictions from the effective Lagrangian model of Bauer, Stech and Wirbel[1] (BSW) and the $1/N_C$ model of Lee[8]. These predictions agree well with our measurements within errors. As has been emphasized by many authors, final state interactions can alter predictions in individual decay modes. Therefore it is better to examine predictions for several final states to look for broad agreement between models and predictions, as we have done here.

We would like to acknowledge useful discussions with E. L. Berger, I. I. Bigi and B. Stech. We gratefully acknowledge the assistance of the staff of Fermilab and of all the participating institutions. This research was supported by the U. S. Department of Energy, by the National Science Foundation, by the Natural Science and Engineering Research Council of Canada through the Institute of Particle Physics, by the National Research Council of Canada and by the Brazilian Conselho Nacional de Desenvolvimento Científico e Tecnológico.

REFERENCES

[a] Now at Cornell University, Ithaca, NY, USA.

[b] Now at CERN, Geneva, Switzerland.

[c] Now at Electro Magnetic Applications, Inc., Denver, CO, USA.

[d] Now at Nichols Research, Colorado Springs, CO, USA.

[e] Now at Harvard University, Cambridge, MA, USA.

[f] Now at the Univ. of California, Santa Barbara, CA, USA.

[g] Now at SLAC, Stanford, CA, USA.

[h] Now at Mainz University, Mainz, Germany.

[i] Now at the Univ. of California, Irvine, CA, USA.

[j] Deceased.

[k] Now at Tufts University, Medford, MA, USA.

[*] Operated by the Universities Research Association, Inc. under contract with the United States Department of Energy.

[1] M. Bauer, B. Stech and M. Wirbel, Z. Phys. **C34**, 103 (1987).

[2] A. N. Kamal, Phys. Rev. **D33**, 1344 (1986).

[3] J. R. Raab et al., Phys. Rev. **D37**, 2391 (1988) and additional references therein.

[4] K. Hikasa et al., Phys. Rev. **D45** (1992).

[5] J. Adler et al., Phys. Lett. **196B**, 107 (1987).

[6] M. Diakonou and F. Diakonos, Phys. Lett. **216B**, 436 (1989).

[7] J. C. Anjos et al., Phys. Rev. **D46**, 1941 (1992).

[8] D. Lee, private communication (paper in preparation).
D. Lee, Phys. Lett. **275B**, 469 (1992) and erratum Phys. Lett. **277B**, 529 (1992) describe his model for D→P + P decays.

FIGURES

FIG. 1. Mass plots for a) the $D^+ \rightarrow K^- \pi^+ \pi^+$ mode, b) the $D^0 \rightarrow K^- \pi^+ \pi^0$ mode and c) the $D^0 \rightarrow \overline{K}^0 \pi^+ \pi^-$ mode.

FIG. 2. Dalitz plots for a) the $D^+ \rightarrow K^- \pi^+ \pi^+$ events in the signal region, b) the $D^+ \rightarrow K^- \pi^+ \pi^+$ events in the background region and c) the $D^+ \rightarrow K^- \pi^+ \pi^+$ simulated background.

FIG. 3. Dalitz plots for a) $D^0 \rightarrow K^- \pi^+ \pi^0$ events in the signal region and b) $D^0 \rightarrow \overline{K}^0 \pi^+ \pi^-$ events in the signal region.

FIG. 4. Projections of the Dalitz plots on to the three axes for a) the $D^+ \rightarrow K^- \pi^+ \pi^+$ mode, b) the $D^0 \rightarrow K^- \pi^+ \pi^0$ mode and c) the $D^0 \rightarrow \overline{K}^0 \pi^+ \pi^-$ mode.
The solid line represents the data, the dotted line is a projection of the fitted density.

TABLES

TABLE I. Relative amplitudes and phases from the fits to the Dalitz plot for the $D^+ \to K^-\pi^+\pi^+$ mode.

Resonance	Amplitude (c_k)	Phase (θ_k) (degrees)	Fit fraction	Branching ratio (%)
Non-resonant $K^-\pi^+\pi^-$	1.	0.	0.838	$6.7 \pm 0.7 \pm 2.2$
$\overline{K}^*(892)^0\pi^+$	0.78 ± 0.02	-60 ± 3	0.170 ± 0.009	$2.0 \pm 0.2 \pm 0.4$
$\overline{K}_0^*(1430)^0\pi^+$	0.53 ± 0.02	132 ± 2	0.248 ± 0.019	$3.0 \pm 0.4 \pm 0.2$
$\overline{K}^*(1680)^0\pi^+$	0.47 ± 0.03	-51 ± 4	0.030 ± 0.004	$0.9 \pm 0.2 \pm 0.4$

TABLE II. Relative amplitudes and phases from the fits to the Dalitz plot for the $D^0 \to K^-\pi^+\pi^0$ mode.

Resonance	Amplitude (c_k)	Phase (θ_k) (degrees)	Fit fraction	Branching ratio (%)
Non-resonant $K^-\pi^+\pi^0$	1.	0.	0.036	$0.41 \pm 0.04 \pm 0.2$
$\overline{K}^*(892)^0\pi^0$	3.19 ± 0.20	167 ± 9	0.142 ± 0.018	$2.4 \pm 0.4 \pm 0.4$
$K^*(892)^-\pi^+$	2.96 ± 0.19	-112 ± 9	0.084 ± 0.011	$2.8 \pm 0.5 \pm 0.4$
$K^-\rho(770)^+$	8.56 ± 0.26	40 ± 7	0.647 ± 0.039	$7.3 \pm 0.8 \pm 1.7$

TABLE III. Relative amplitudes and phases from the fits to the Dalitz plot for the $D^0 \to \overline{K}^0\pi^+\pi^-$ mode.

Resonance	Amplitude (c_k)	Phase (θ_k) (degrees)	Fit fraction	Branching ratio (%)
Non-resonant $\overline{K}^0\pi^+\pi^-$	1.	0.	0.263	$1.4 \pm 0.13 \pm 0.22$
$K^*(892)^-\pi^+$	2.31 ± 0.23	109 ± 9	0.480 ± 0.097	$3.9 \pm 0.9 \pm 1.0$
$\overline{K}^0\rho(770)^0$	1.59 ± 0.19	-123 ± 12	0.215 ± 0.051	$1.2 \pm 0.3 \pm 0.2$

TABLE IV. Comparison to Mark III results[5] and the BSW[1] and Lee[8] models.

Decay Mode	E691 B.R. (%)	Mark III B.R. (%)	BSW prediction (%)	Lee prediction (%)
$K^-\pi^+\pi^+$ final state:				
$D^+ \to (K^-\pi^+\pi^+)_{NR}$	$6.7 \pm 0.7 \pm 2.2$	$7.2 \pm 0.6 \pm 1.8$	—	—
$D^+ \to \overline{K}^*(892)^0\pi^+$	$2.0 \pm 0.2 \pm 0.4$	$1.8 \pm 0.2 \pm 1.0$	0.3	2.4
$D^+ \to \overline{K}_0^*(1430)^0\pi^+$	$3.0 \pm 0.4 \pm 0.2$	—	—	—
$D^+ \to \overline{K}^*(1680)^0\pi^+$	$0.9 \pm 0.2 \pm 0.4$	—	—	—
$K^-\pi^+\pi^0$ final state:				
$D^0 \to (K^-\pi^+\pi^0)_{NR}$	$0.41 \pm 0.04 \pm 0.18$	$1.2 \pm 0.2 \pm 0.6$	—	—
$D^0 \to \overline{K}^*(892)^0\pi^0$	$2.4 \pm 0.4 \pm 0.4$	$2.6 \pm 0.3 \pm 0.7$	1.4 - 3.9	0.73
$D^0 \to K^*(892)^-\pi^+$	$2.8 \pm 0.5 \pm 0.4$	$4.9 \pm 0.7 \pm 1.5$	3.7 - 9.1	4.9
$D^0 \to K^-\rho^+$	$7.3 \pm 0.8 \pm 1.7$	$10.8 \pm 0.4 \pm 1.7$	12.5 - 13.8	8.7
$\overline{K}^0\pi^+\pi^-$ final state:				
$D^0 \to (\overline{K}^0\pi^+\pi^-)_{NR}$	$1.4 \pm 0.13 \pm 0.22$	$2.1 \pm 0.3 \pm 0.7$	—	—
$D^0 \to K^*(892)^-\pi^+$	$3.9 \pm 0.9 \pm 1.0$	$5.3 \pm 0.4 \pm 1.0$	3.7 - 9.1	4.9
$D^0 \to \overline{K}^0\rho(770)^0$	$1.2 \pm 0.3 \pm 0.2$	$0.8 \pm 0.1 \pm 0.5$	0.9 - 1.1	0.38

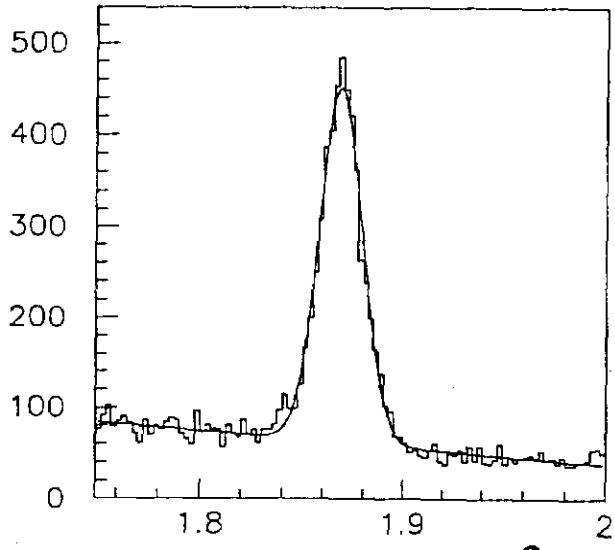

$m_{K^-\pi^+\pi^+}$ (GeV/c^2)

a)

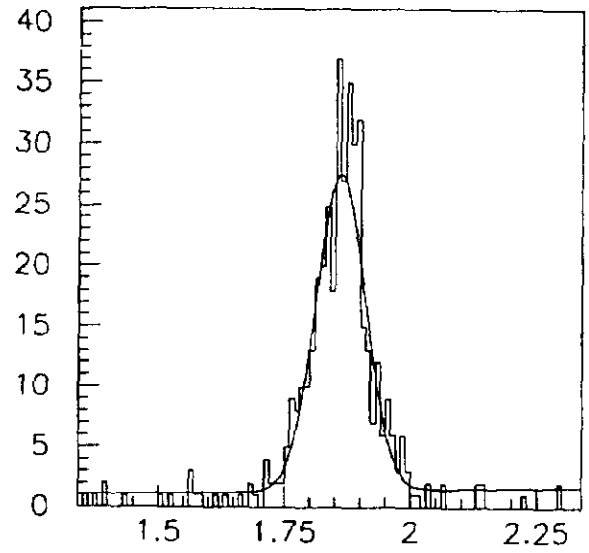

$m_{K^-\pi^+\pi^0}$(GeV/c^2)

b)

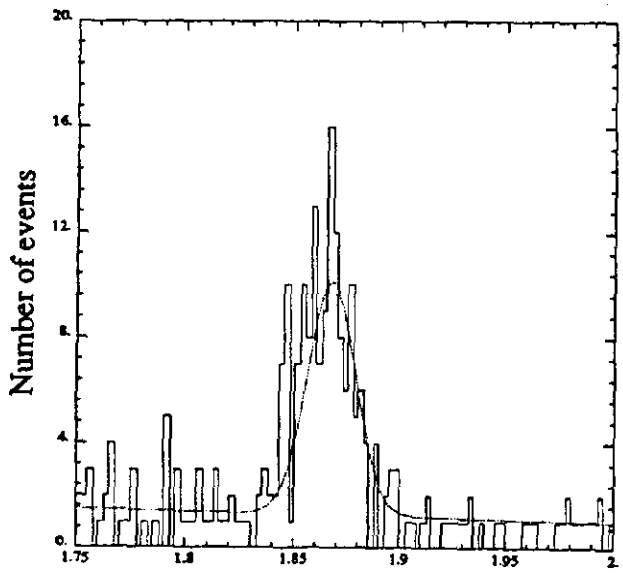

$m_{K^0_S\pi^+\pi^-}$ (GeV/c^2)

c)

Fig. 1

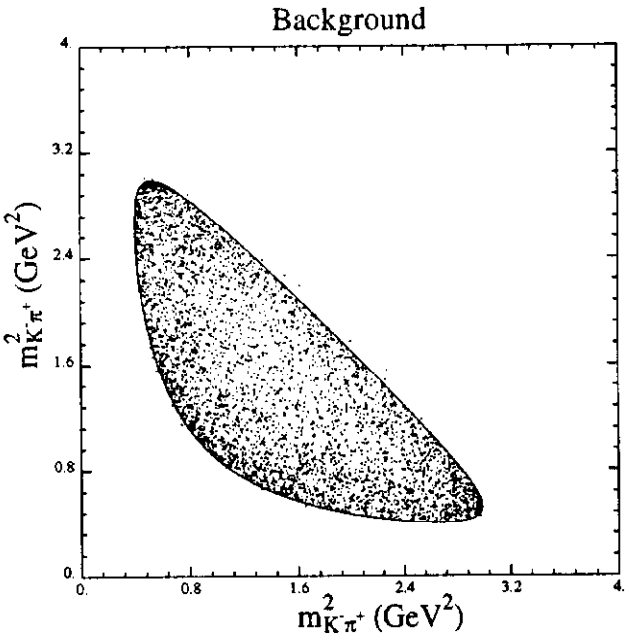
Background
$m^2_{K^-\pi^+}$ (GeV^2)
$m^2_{K^-\pi^+}$ (GeV^2)
0
0.8
1.6
2.4
3.2
4

b)

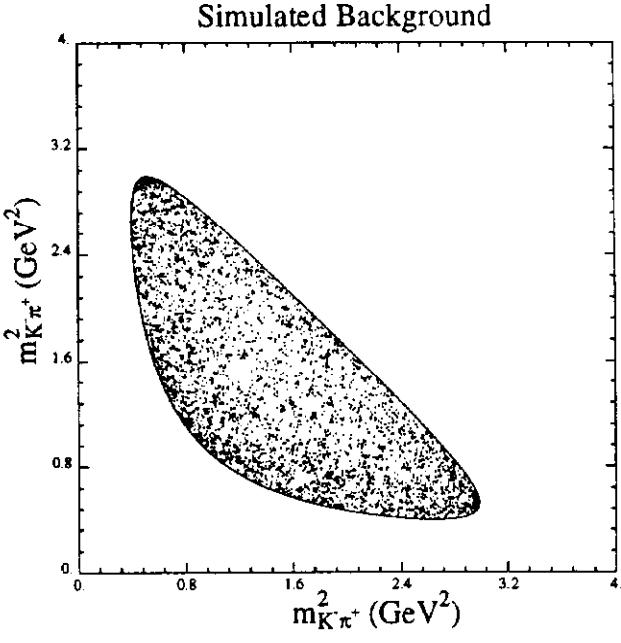
Simulated Background
$m^2_{K^-\pi^+}$ (GeV^2)
$m^2_{K^-\pi^+}$ (GeV^2)
0
0.8
1.6
2.4
3.2
4

c)

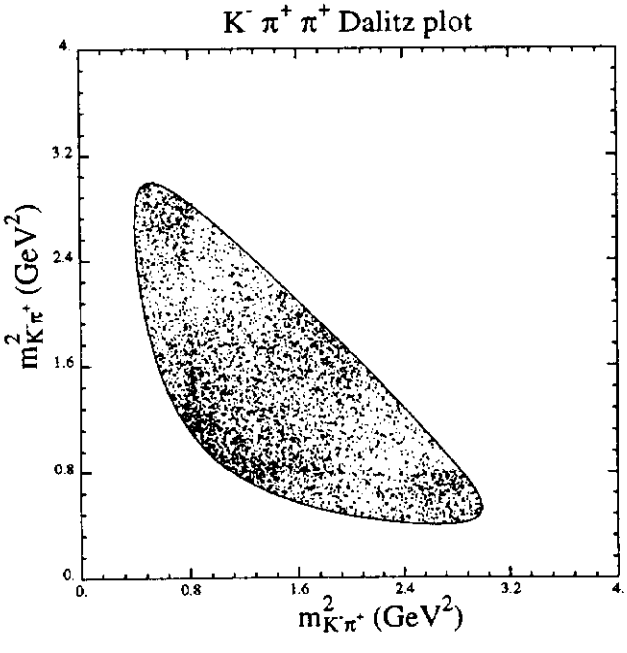
$K^- \pi^+ \pi^+$ Dalitz plot
$m^2_{K^-\pi^+}$ (GeV^2)
$m^2_{K^-\pi^+}$ (GeV^2)
0
0.8
1.6
2.4
3.2
4

a)

Fig. 2.

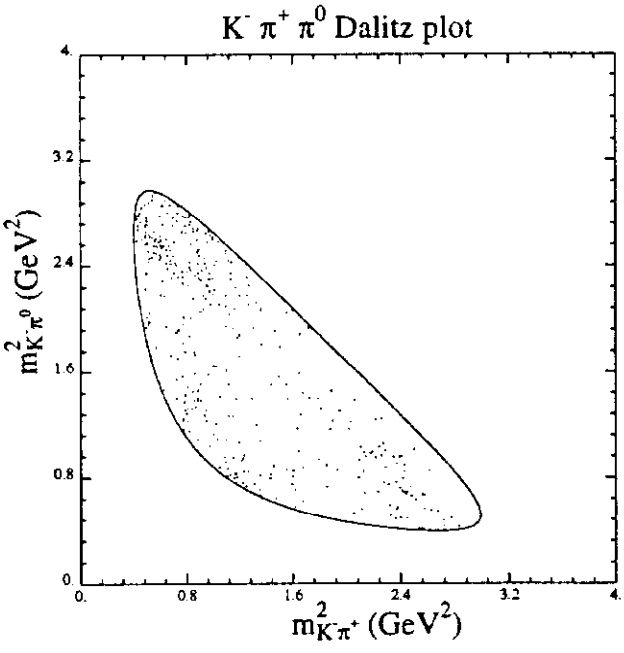
$K^- \pi^+ \pi^0$ Dalitz plot
$m^2_{K^-\pi^0}$ (GeV^2)
$m^2_{K^-\pi^+}$ (GeV^2)
0
0.8
1.6
2.4
3.2
4

a)

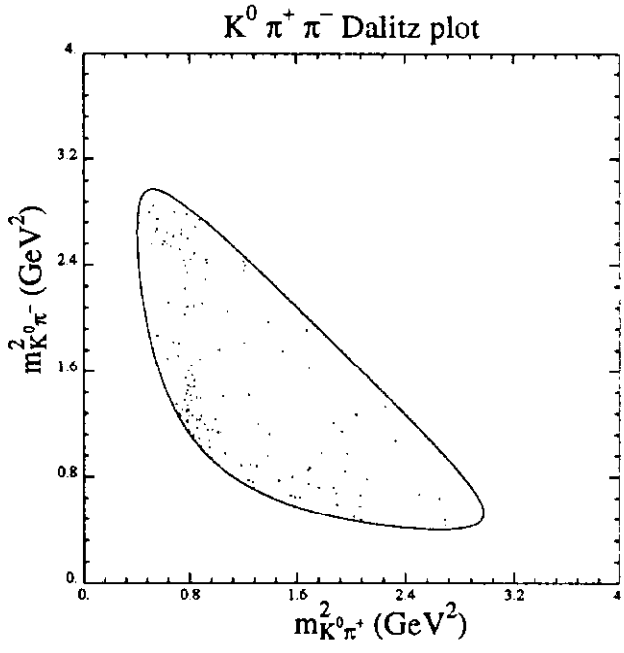
$K^0 \pi^+ \pi^-$ Dalitz plot
$m^2_{K^0\pi^-}$ (GeV^2)
$m^2_{K^0\pi^+}$ (GeV^2)
0
0.8
1.6
2.4
3.2
4

b)

Fig. 3.)

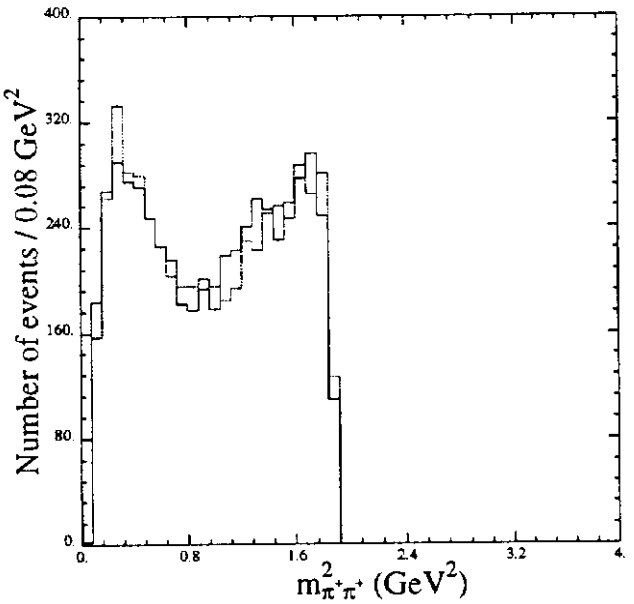
Number of events / 0.08 GeV^2
$m^2_{\pi^+\pi^+}$ (GeV^2)

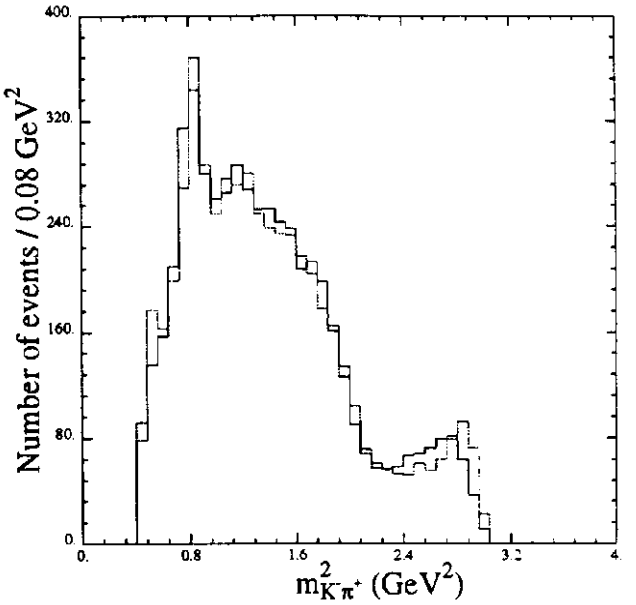
Number of events / 0.08 GeV^2
$m^2_{K^-\pi^+}$ (GeV^2)

Fig. 4a)

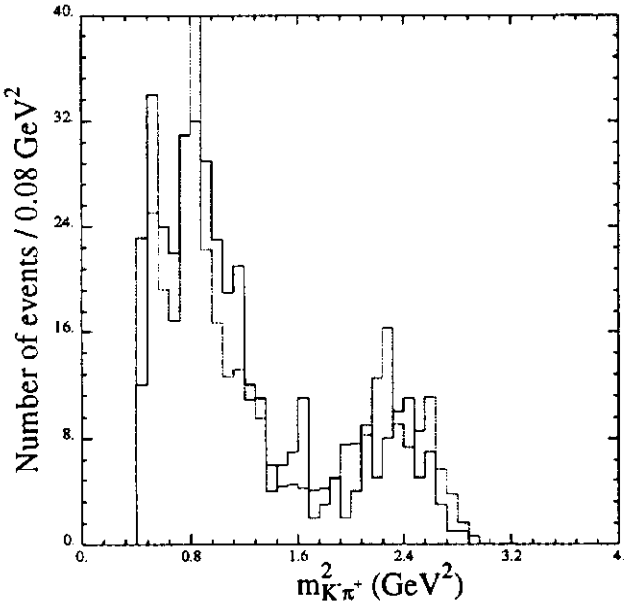
Number of events / 0.08 GeV^2
$m^2_{K^-\pi^+}$ (GeV^2)

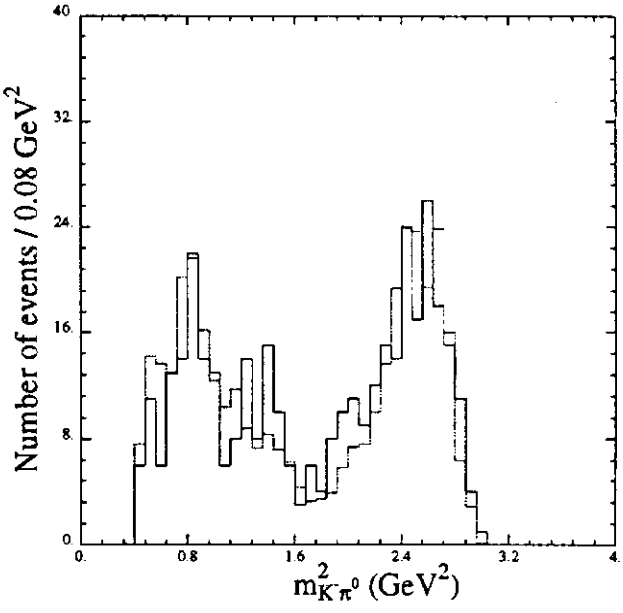
Number of events / 0.08 GeV^2
$m^2_{K^-\pi^0}$ (GeV^2)

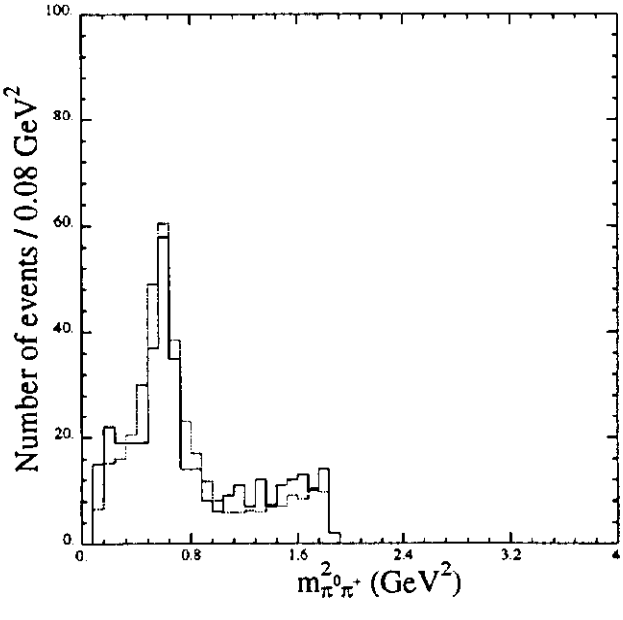
Number of events / 0.08 GeV^2
$m^2_{\pi^0\pi^+}$ (GeV^2)

Fig. 4b)

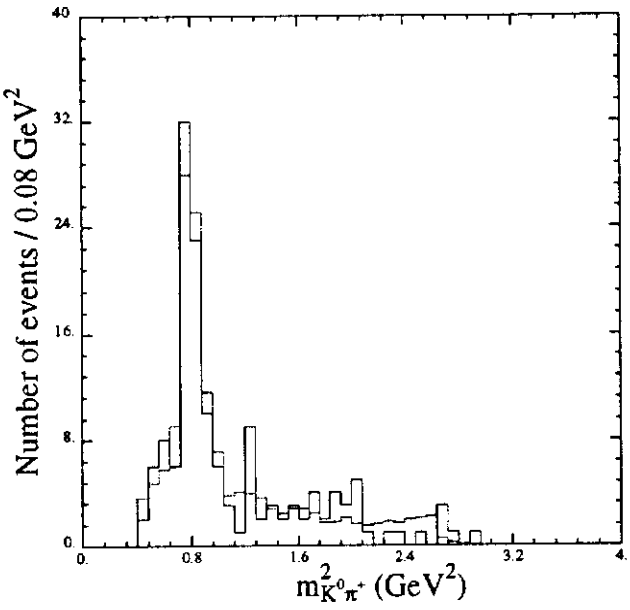
Number of events / 0.08 GeV^2
$m^2_{K^0\pi^+}$ (GeV^2)

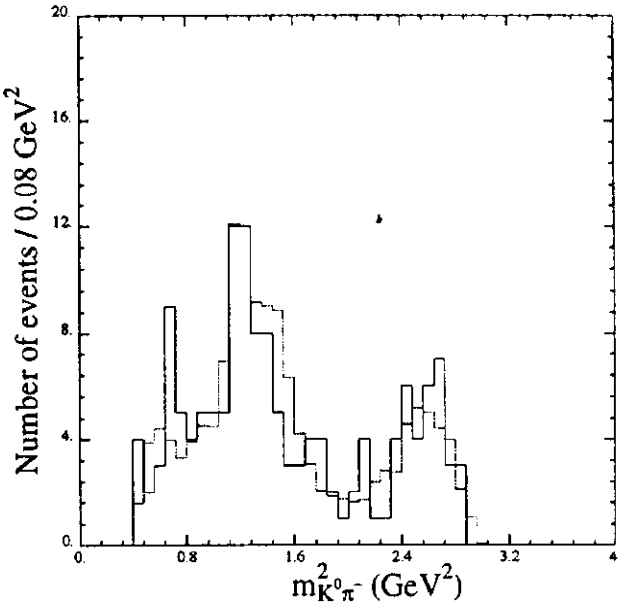
Number of events / 0.08 GeV^2
$m^2_{K^0\pi^-}$ (GeV^2)

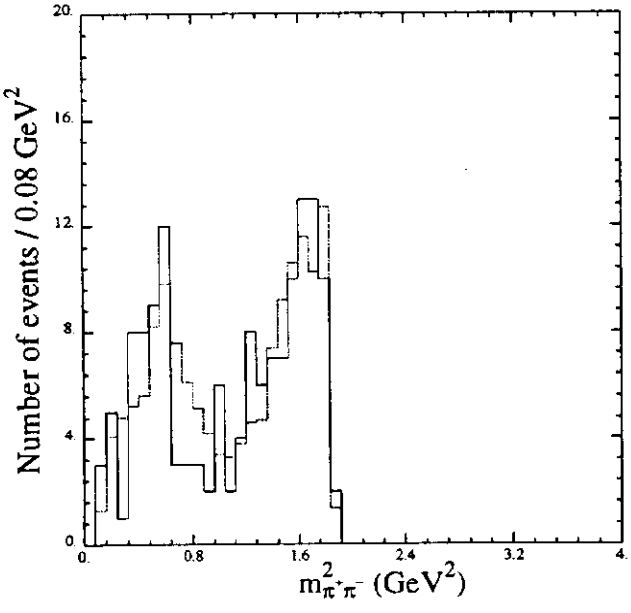
Number of events / 0.08 GeV^2
$m^2_{\pi^+\pi^-}$ (GeV^2)

Fig. 4c)